

Mechanistic Studies of the O₂-Dependent Aliphatic Carbon–Carbon Bond Cleavage Reaction of a Nickel Enolate Complex

Lisa M. Berreau,^{*,†} Tomasz Borowski,[‡] Katarzyna Grubel,[†] Caleb J. Allpress,[†] Jeffrey P. Wikstrom,[§] Meaghan E. Germain,[§] Elena V. Rybak-Akimova,[§] and David L. Tierney[⊥]

[†]Department of Chemistry and Biochemistry, Utah State University, Logan, Utah 84322-0300, United States,

[‡]Institute for Catalysis and Surface Chemistry, Polish Academy of Science, Krakow, Poland,

[§]Department of Chemistry, Tufts University, Boston, Massachusetts 02155, United States, and

[⊥]Department of Chemistry and Biochemistry, Miami University, Oxford, Ohio 45056, United States

Received September 1, 2010

The mononuclear nickel(II) enolate complex [(6-Ph₂TPA)Ni(PhC(O)C(OH)C(O)Ph)ClO₄ (**I**) was the first reactive model complex for the enzyme/substrate (ES) adduct in nickel(II)-containing acireductone dioxygenases (ARDs) to be reported. In this contribution, the mechanism of its O₂-dependent aliphatic carbon–carbon bond cleavage reactivity was further investigated. Stopped-flow kinetic studies revealed that the reaction of **I** with O₂ is second-order overall and is ~80 times slower at 25 °C than the reaction involving the enolate salt [Me₄N][PhC(O)C(OH)C(O)Ph]. Computational studies of the reaction of the anion [PhC(O)C(OH)C(O)Ph][−] with O₂ support a hydroperoxide mechanism wherein the first step is a redox process that results in the formation of 1,3-diphenylpropanetrione and HOO[−]. Independent experiments indicate that the reaction between 1,3-diphenylpropanetrione and HOO[−] results in oxidative aliphatic carbon–carbon bond cleavage and the formation of benzoic acid, benzoate, and CO:CO₂ (~12:1). Experiments in the presence of a nickel(II) complex gave a similar product distribution, albeit benzil [PhC(O)C(O)Ph] is also formed, and the CO:CO₂ ratio is ~1.5:1. The results for the nickel(II)-containing reaction match those found for the reaction of **I** with O₂ and provide support for a trione/HOO[−] pathway for aliphatic carbon–carbon bond cleavage. Overall, **I** is a reasonable structural model for the ES adduct formed in the active site of Ni^{II}ARD. However, the presence of phenyl appendages at both C(1) and C(3) in the [PhC(O)C(OH)C(O)Ph][−] anion results in a reaction pathway for O₂-dependent aliphatic carbon–carbon bond cleavage (via a trione intermediate) that differs from that accessible to C(1)–H acireductone species. This study, as the first detailed investigation of the O₂ reactivity of a nickel(II) enolate complex of relevance to Ni^{II}ARD, provides insight toward understanding the chemical factors involved in the O₂ reactivity of metal acireductone species.

Introduction

Metalloenzyme-catalyzed dioxygenase reactions result in the incorporation of both atoms of an O₂ molecule into a substrate. Extensive studies of the aromatic carbon–carbon bond cleavage reactions promoted by catechol and Rieske dioxygenases have given insight into the reaction mechanisms of these enzymes.¹ However, considerably less is known regarding the mechanistic pathways of metalloenzyme-catalyzed

dioxygenase reactions involving aliphatic carbon–carbon bond cleavage. These systems involve the reaction between a metal-coordinated enolate substrate and O₂ and are catalyzed by enzymes belonging to the cupin superfamily² of proteins: β-diketone dioxygenase (Dke1),³ a β-diketone cleaving oxygenase from *Burkholderia xenovorans* (*Bxe_A2876*),⁴ and the CO-releasing enzymes quercetin 2,3-dioxygenase⁵ and acireductone dioxygenase (ARD).⁶ While Dke1 and *Bxe_A2876* are nonheme iron enzymes, quercetinase enzymes have been shown to be active with a variety of different metal ions.⁷ In the absence of enzyme, the substrate for the

*To whom correspondence should be addressed. E-mail: lisa.berreau@usu.edu. Phone: (435) 797-1625. Fax: (435) 797-3390.

(1) Bugg, T. D. H.; Ramaswamy, S. *Curr. Opin. Chem. Biol.* **2008**, *12*, 134–140.

(2) Dunwell, J. M.; Purvis, A.; Khuri, S. *Phytochemistry* **2004**, *65*, 7–17.

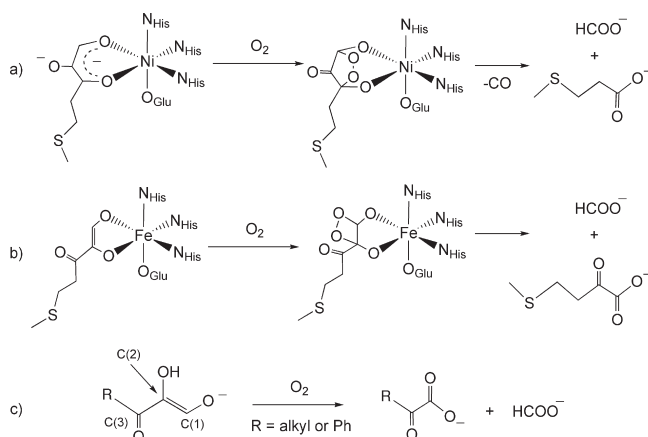
(3) (a) Straganz, G. D.; Diebold, A. R.; Egger, S.; Nidetzky, B.; Solomon, E. I. *Biochemistry* **2010**, *49*, 996–1004. (b) Leitgeb, S.; Straganz, G. D.; Nidetzky, B. *Biochem. J.* **2009**, *418*, 403–411. (c) Straganz, G. D.; Nidetzky, B. *J. Am. Chem. Soc.* **2005**, *127*, 12306–12314. (d) Straganz, G. D.; Hofer, H.; Steiner, W.; Nidetzky, B. *J. Am. Chem. Soc.* **2004**, *126*, 12202–12203. (e) Straganz, G. D.; Glieder, A.; Brecker, L.; Ribbons, D. W.; Steiner, W. *Biochem. J.* **2003**, *369*, 573–581.

(4) Leitgeb, S.; Straganz, G. D.; Nidetzky, B. *FEBS J.* **2009**, *276*, 5983–5997.

(5) (a) Baráth, G.; Kaizer, J.; Speier, G.; Párkányi, L.; Kuzmann, E.; Vértés, A. *Chem. Commun.* **2009**, 3630–3632 and references cited therein. (b) Steiner, R. A.; Kalk, K. H.; Dijkstra, B. W. *Proc. Natl. Acad. Sci. U.S.A.* **2002**, *99*, 16625–16630.

(6) Pochapsky, T. C.; Ju, T.; Dang, M.; Beaulieu, R.; Pagani, G. M.; OuYang, B. In *Metal Ions in Life Sciences*; Sigel, A., Sigel, H., Sigel, R. K. O., Eds.; Wiley-VCH: Weinheim, Germany, 2007; Vol. 2, pp 473–498.

Scheme 1



DkeI enzyme (a β -diketone) is stable with respect to O_2 . This is in contrast to the chemistry of acireductone anions, which are O_2 reactive in the absence of enzyme. ARD enzymes are also a distinct member of this group in that, depending on the metal ion content of the enzyme, different chemical reactions are catalyzed.⁸ As shown in Scheme 1, with Ni^{II} as the active site metal ion, the acireductone substrate is proposed to coordinate as a 1,3-enediolate-type ligand with a deprotonated C(2)-hydroxyl moiety (Scheme 1a).⁹ This coordination motif is suggested to lead to oxidative C(1)-C(2) and C(2)-C(3) bond cleavage and the formation of carbon monoxide and carboxylate products. For the iron(II)-containing enzyme, enediolate coordination is proposed to involve a five-membered chelate ring (Scheme 1b).⁹ The products of the Fe^{II} ARD-catalyzed reaction result from oxidative C(1)-C(2) bond cleavage and are an α -keto carboxylate and formate. In the absence of enzyme, the reaction of an acireductone anion having a C(3) alkyl or aryl substituent with O_2 yields products that are identical with those generated in the Fe^{II} ARD-promoted reaction (Scheme 1c).⁶

Very little is known regarding the mechanistic pathway of O_2 reactivity and CO release involving the proposed Ni^{II} ARD enzyme/substrate (ES) adduct. Computational studies show that the reaction of a simple acireductone monoanion with O_2 likely proceeds via a radical pathway.¹⁰ However, the influence of a metal center on this reaction remains to be elucidated. We

have previously reported the only nickel(II) enolate complexes of relevance to the Ni^{II} ARD ES adduct.¹¹⁻¹⁴ A mononuclear nickel(II) complex, $[(6-Ph_2TPA)Ni(PhC(O)C(OH)C(O)Ph)]ClO_4$ (**I**), was generated, and its reactivity with O_2 was investigated as a function of the protonation level of the enolate ligand.^{11,14} In a reaction wherein **I** is treated with 1 equiv of base, loss of the chelate ligand occurs and a nickel(II) enediolate cluster is generated.¹² This cluster undergoes a reaction with O_2 to yield CO, the dibenzoate complex $[(6-Ph_2TPA)Ni(O_2CPh)_2(H_2O)]$ (**II**), and the organic byproduct benzil (Scheme 2).^{11a,12} This reaction is similar to that found for a trinuclear nickel(II) complex that we have also previously isolated and characterized.¹³ Treatment of **I** with O_2 in the absence of base results in the formation of a nickel(II) monobenzoate complex $[(6-Ph_2TPA)Ni(O_2CPh)]ClO_4$ (**III**); Scheme 2),^{11b} benzoic acid, CO, and benzil. The reaction of the enolate salt $[Me_4N][PhC(O)C(OH)C(O)Ph]$ with O_2 gives tetramethylammonium benzoate, benzoic acid, and CO (Scheme 2, bottom).^{11b,14} The levels of ^{18}O incorporation in the benzoic acid/benzoate products [both nickel(II)-coordinated and free organics] are similar for reactions involving the anion $[PhC(O)C(OH)C(O)Ph]^-$ (**I**).^{11b,14} These combined results for **I** and the salt $[Me_4N][PhC(O)C(OH)C(O)Ph]$ indicate that the regioselectivity of the aliphatic carbon-carbon bond cleavage reaction is not influenced by the presence of the nickel(II) center because the C(1)-C(2) and C(2)-C(3) bonds are oxidatively cleaved in both reactions (Scheme 2). The formation of benzil in the reaction involving **I** suggests that a reaction pathway involving a 1,3-diphenylpropanetrione intermediate may be operative (pathway B in Scheme 3) instead of a pathway involving a nickel(II)-coordinated cyclic peroxide species (pathway A in Scheme 3). In the proposed pathway B, a nickel(II) complex could act as a Lewis acid to promote phenyl or benzoyl migration in the 1,3-diphenylpropanetrione intermediate.

In the research described herein, we have performed studies to further investigate the O_2 reactivity of **I**. The experiments reported include (1) kinetic studies of the reactions of **I**, and the salt $[Me_4N][PhC(O)C(OH)C(O)Ph]$, with O_2 , (2) a computational investigation of the reaction pathway of **I** with O_2 , and (3) an evaluation of the chemistry of 1,3-diphenylpropanetrione in the presence of a nickel(II) solvate complex, $[(6-Ph_2TPA)Ni(CH_3CN)(H_2O)](ClO_4)_2 \cdot H_2O$ (**IV**).

Experimental Section

General Methods. All reagents and solvents were obtained from commercial sources and were used as received unless otherwise noted. Solvents were dried according to published procedures and were distilled under N_2 prior to use.¹⁵ Air-sensitive procedures were performed in a MBraun Unilab glovebox or a Vacuum Atmospheres MO-20 glovebox under a N_2 atmosphere. The trione 1,3-diphenylpropanetrione was purchased from TCI America and was used as received after checking for purity by 1H NMR. The ligand 6- Ph_2 TPA, the nickel(II) complex $[(6-Ph_2TPA)Ni(PhC(O)C(OH)C(O)Ph)]ClO_4$ (**I**), and

(7) (a) Oka, T.; Simpson, F. J. *Biochem. Biophys. Res. Commun.* **1971**, *43*, 1-5. (b) Oka, T.; Simpson, F. J.; Krishnamurthy, N. G. *Can. J. Microbiol.* **1972**, *18*, 493-508. (c) Hund, H. K.; Breuer, J.; Lingens, F.; Huttermann, J.; Kapp, R.; Fetzner, S. *Eur. J. Biochem.* **1999**, *263*, 871-878. (d) Tranchimand, S.; Ertel, G.; Gaydou, V.; Gaudin, C.; Tron, T.; Iacazio, G. *Biochimie* **2008**, *90*, 781-789. (e) Kooter, I. M.; Steiner, R. A.; Dijkstra, B. W.; van Noort, P. I.; Egmond, M. R.; Huber, M. *Eur. J. Biochem.* **2002**, *269*, 2971-2979. (f) Fusetti, F.; Schröter, K. H.; Steiner, R. A.; van Noort, P. I.; Pijning, T.; Rozeboom, H. J.; Kalk, K. H.; Egmond, M. R.; Dijkstra, B. W. *Structure* **2002**, *10*, 259-268. (g) Gopal, B.; Madan, L. L.; Betz, S. F.; Kossiakoff, A. A. *Biochemistry* **2005**, *44*, 193-201. (h) Schaab, M. R.; Barney, B. M.; Francisco, W. A. *Biochemistry* **2006**, *45*, 1009-1016. (i) Merckens, H.; Kapp, R.; Jakob, R. P.; Schmid, F. X.; Fetzner, S. *Biochemistry* **2008**, *47*, 12185-12196.

(8) Dai, Y.; Wensink, P. C.; Abeles, R. H. *J. Biol. Chem.* **1999**, *274*, 1193-1195.

(9) Ju, T.; Goldsmith, R. B.; Chai, S. C.; Maroney, M. J.; Pochapsky, S. S.; Pochapsky, T. C. *J. Mol. Biol.* **2006**, *363*, 823-834.

(10) Borowski, T.; Bassan, A.; Siegbahn, P. E. M. *THEOCHEM* **2006**, *772*, 89-92.

(11) (a) Szajna, E.; Arif, A. M.; Berreau, L. M. *J. Am. Chem. Soc.* **2005**, *127*, 17186-17187. (b) Szajna-Fuller, E.; Rudzka, K.; Arif, A. M.; Berreau, L. M. *Inorg. Chem.* **2007**, *46*, 5499-5507.

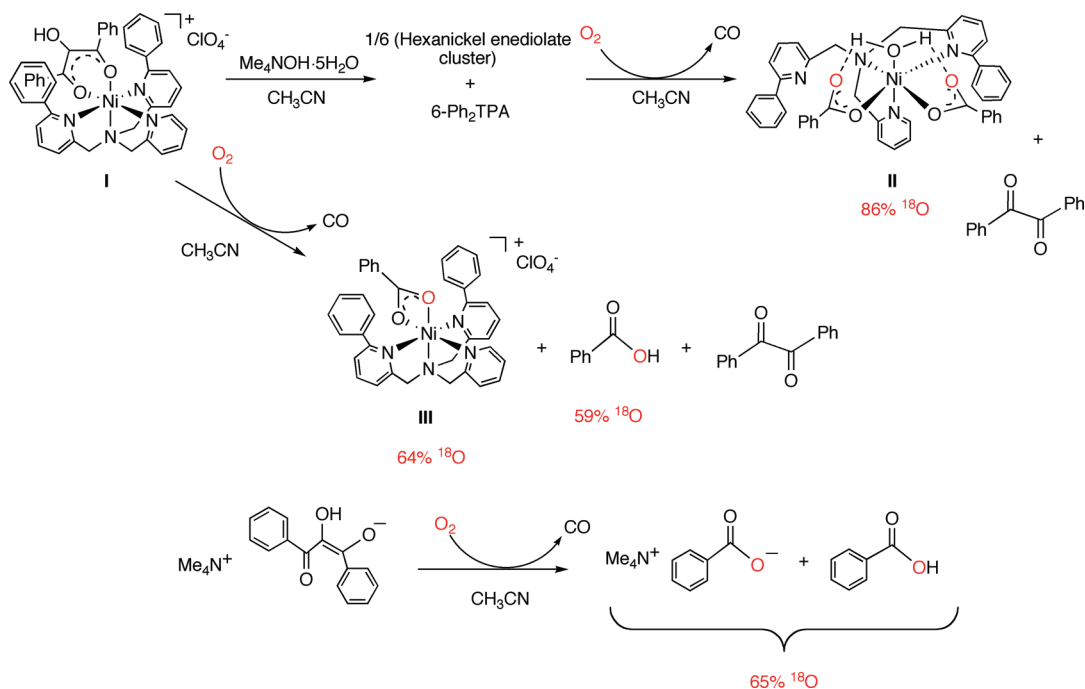
(12) Rudzka, K.; Grubel, K.; Arif, A. M.; Berreau, L. M. *Inorg. Chem.* **2010**, *49*, 7623-7625.

(13) Rudzka, K.; Arif, A. M.; Berreau, L. M. *Inorg. Chem.* **2008**, *47*, 10832-10840.

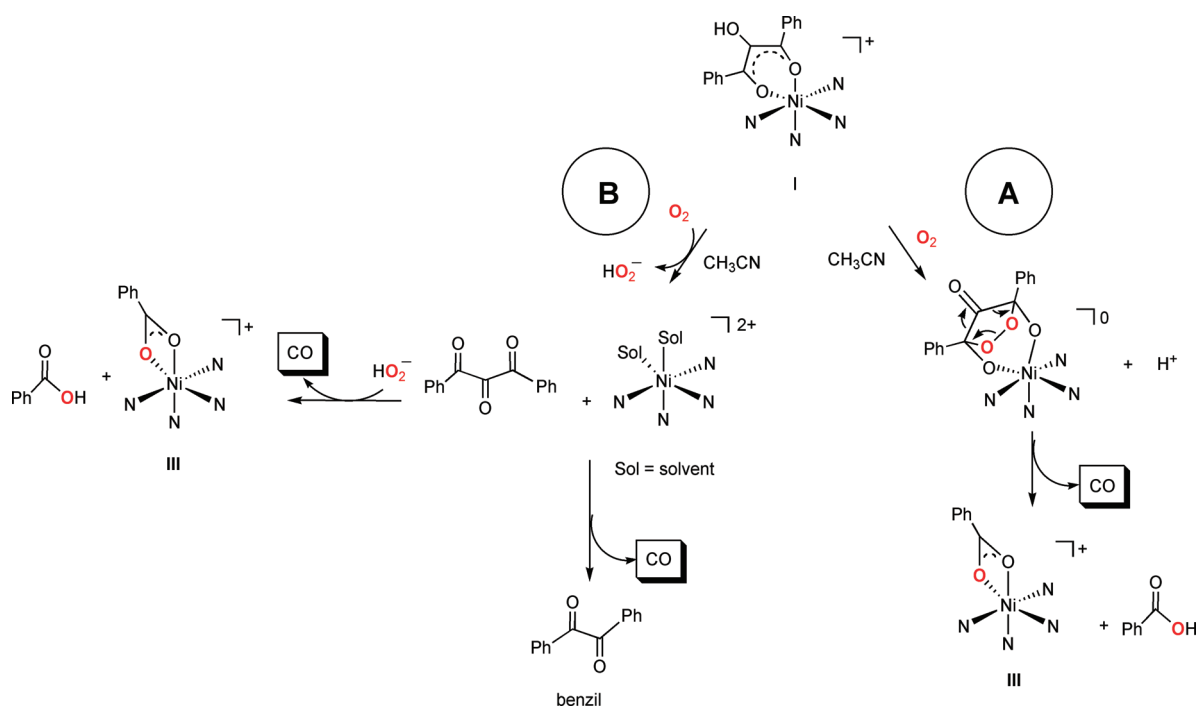
(14) Grubel, K.; Fuller, A. L.; Chambers, B. M.; Arif, A. M.; Berreau, L. M. *Inorg. Chem.* **2010**, *49*, 1071-1081.

(15) Armarego, W. L. F.; Perrin, D. D. *Purification of Laboratory Chemicals*, 4th ed.; Butterworth-Heinemann: Boston, MA, 1996.

Scheme 2



Scheme 3



the salt $[\text{Me}_4\text{N}][\text{PhC}(\text{O})\text{C}(\text{OH})\text{C}(\text{O})\text{Ph}]$ were prepared as previously described.^{11,16}

Physical Methods. ^1H NMR spectra of diamagnetic compounds were collected on either a JEOL ECX-300 NMR or a Bruker ARX-400 spectrometer. ^1H NMR data for paramagnetic complexes of nickel(II) were collected using a Bruker ARX-400

spectrometer as previously described.¹⁷ Chemical shifts (in ppm) are reported relative to the residual solvent peak in CHD_2CN [^1H , 1.94 (quintet) ppm]. Gas chromatography–mass spectrometry (GC–MS) data were obtained using a Shimadzu QP5000 with an Alltech EC-5 column and ultrahigh-purity helium as the carrier gas. CO formation was determined qualitatively via the PdCl_2 method¹⁸ or using an Agilent 3000A Micro gas chromatograph, the latter of which also enabled identification of CO_2 . The reported ratio of CO/CO_2 in the headspace gas of the reactions is based on GC peak integration and an independently prepared calibration curve developed for CO/CO_2 mixtures. Fourier transform infrared (FTIR) spectra were recorded on a Shimadzu

(16) Makowska-Grzyska, M. M.; Szajna, E.; Shipley, C.; Arif, A. M.; Mitchell, M. H.; Halfen, J. A.; Berreau, L. M. *Inorg. Chem.* **2003**, *42*, 7472–7488.

(17) Szajna, E.; Dobrowolski, P.; Fuller, A. L.; Arif, A. M.; Berreau, L. M. *Inorg. Chem.* **2004**, *43*, 3988–3997.

FTIR-8400 spectrometer. Elemental analyses were performed by Atlantic Microlabs, Inc., Norcross, GA.

Stopped-Flow Kinetic Studies. Measurements were performed using either a SF-61DX2 or a SF-43 multimixing anaerobic cryogenic stopped-flow instrument (TgK Scientific, formerly Hi-Tech Scientific, Salisbury, Wiltshire, U.K.) combined with either a Hi-Tech Scientific KinetaScan diode-array or a J&M diode-array spectrophotometer. All manipulations of **I** and [Me₄N][PhC(O)C(OH)C(O)Ph] and their solutions were performed inside an argon-filled glovebox. For stopped-flow kinetic studies involving **I**, solutions of a known concentration of the complex were prepared and then placed in a Hamilton gastight syringe, which was loaded into the stopped-flow sample handling unit. To generate [Me₄N][PhC(O)C(OH)C(O)Ph], solid Me₄NOH·5H₂O was fully dissolved in dry acetonitrile (2 mM). A CH₃CN solution containing an equimolar amount of PhC(O)CH(OH)C(O)Ph was then added, which resulted in the formation of a bright-orange solution. After 30 min of stirring, the solution of [Me₄N][PhC(O)C(OH)C(O)Ph] was transferred to a gastight syringe and diluted. Saturated solutions of O₂ in CH₃CN (8.2 mM) were prepared by bubbling dry O₂ through an argon-saturated solvent. Solutions containing lower concentrations of O₂ were prepared by dilution of the 8.2 mM solution with argon-saturated CH₃CN using gastight syringes. For the kinetic runs of the O₂ reactions of **I** and [Me₄N][PhC(O)C(OH)C(O)Ph] used to generate the Eyring plot, the final concentrations were 0.3 mM (enolate complex or salt) and 4.1 mM (O₂). Data analysis was performed with the IS-2 or Kinetic Studio Rapid Kinetics Software (TgK Scientific).

Computational Experiments. All calculations were performed by employing hybrid density functional theory with the B3LYP exchange-correlation functional,¹⁹ as implemented in the Jaguar²⁰ quantum chemistry program. Geometry optimizations and frequency calculations were done with a standard valence double- ζ basis set supplemented with a single set of polarization and diffuse functions on non-hydrogen atoms, i.e., 6-31G+*. The solvent corrections were calculated with the self-consistent-field reaction method implemented in Jaguar.²¹ A dielectric constant of 37 and a probe radius of 2.18 Å were used to model the solvent effects due to acetonitrile. The thermal corrections were calculated for room temperature (298.15 K) and a pressure of 1 bar from the Hessian matrix using the standard rigid rotor and harmonic oscillator approximations. The energies reported are thus relative Gibbs free energies that include electronic energies, solvent, and thermal corrections all calculated at the B3LYP/6-31G+* level of theory. The zero energy level corresponds to separated substrates, specifically triplet O₂ and the monoanion [PhC(O)C(OH)C(O)Ph]⁻ (**1**) in the singlet ground state. Structures of all intermediates and TSs were fully optimized, and the character of the stationary point was confirmed by a frequency analysis; i.e., minima and TSs have zero or one imaginary frequency, respectively.

Caution! Perchlorate salts of metal complexes with organic ligands are potentially explosive. Only small amounts of material should be handled with great care.²²

Reaction of 1,3-Diphenylpropanetrione and H₂O₂. 1,3-Diphenylpropanetrione (10 mg, 4.2 × 10⁻⁵ mol) was combined with aqueous H₂O₂ (4.2 μL of 31% solution; 4.2 × 10⁻⁵ mol) in ~1 mL of dry acetonitrile. This produced a yellow solution. The reaction mixture was stirred for 24 h. Sampling of the headspace gas of this reaction mixture indicated the formation of CO/CO₂ in a ~12:1

ratio. ¹H NMR and GC-MS analysis of the products indicated the presence of unreacted 1,3-diphenylpropanetrione (~57%), hydrated 1,3-diphenylpropanetrione (~7%), and benzoic acid (~36%).

Reaction of 1,3-Diphenylpropanetrione and H₂O₂ in the Presence of NEt₃. The reaction mixture described above was prepared. To this solution was added dry Et₃N (5.9 μL, 4.2 × 10⁻⁵ mol). The mixture was then stirred for 24 h. Sampling of the headspace gas of this reaction mixture indicated the formation of CO/CO₂ in a ~12:1 ratio. After this time, the solvent was removed under reduced pressure. ¹H NMR and GC-MS analysis of the products indicated the presence of benzoic acid/[Et₃NH][benzoate] (~70%), unreacted 1,3-diphenylpropanetrione (~30%), and a trace amount of hydrated trione.

Preparation of [(6-Ph₂TPA)Ni(CH₃CN)(H₂O)](ClO₄)₂·H₂O (IV**).** This complex is a solvation analogue of the previously reported [(6-Ph₂TPA)Ni(CH₃CN)(CH₃OH)](ClO₄)₂.¹⁶ An admixture of 6-Ph₂TPA (0.07 mmol) and Ni(ClO₄)₂·6H₂O (0.07 mmol) in CH₃CN (~2 mL), followed by diffusion with diethyl ether, yielded purple crystals (51 mg, 91%). The crystals were crushed and dried under vacuum prior to elemental analysis. Anal. Calcd for C₃₂H₃₃Cl₂N₅NiO₁₀: C, 49.45; H, 4.28; N, 9.01. Found: C, 49.39; H, 4.38; N, 8.92. The ¹H NMR, UV-vis, and FTIR features of this complex match those previously reported for [(6-Ph₂TPA)Ni(CH₃CN)(CH₃OH)](ClO₄)₂.¹⁶

Treatment of IV with 1,3-Diphenylpropanetrione. This reaction was run in the presence and absence of O₂ with no change in the outcome. Complex **IV** (33 mg, 4.2 × 10⁻⁵ mol) was combined with 1,3-diphenylpropanetrione (10 mg, 4.2 × 10⁻⁵ mol) in dry acetonitrile (~2 mL, distilled from CaH₂). The resulting mixture was stirred for 6 h at ambient temperature. Sampling of the headspace gas indicated primarily the formation of CO₂ with only a trace amount of CO (~1:10 CO/CO₂). After 6 h, the solvent was removed under vacuum. The remaining residue was stirred with 1:1 hexanes/ethyl acetate (~3 mL) for 1 h. This resulted in a yellow solution and a pale-purple precipitate. The purple precipitate was determined to be [(6-Ph₂TPA)Ni(sol)₂](ClO₄)₂ (sol = CH₃CN and/or water) by ¹H NMR.¹⁶ Following filtration of the solution through a Celite plug, the filtrate was brought to dryness. The total amount of organic products isolated was ~8 mg. The organic products identified by GC-MS and ¹H NMR were unreacted 1,3-diphenylpropanetrione, hydrated 1,3-diphenylpropanetrione, benzil, and benzoic acid. The combined yield of benzil and benzoic acid in this reaction was ~30–35% (determined by ¹H NMR).

Treatment of IV with 1,3-Diphenylpropanetrione and H₂O₂. Complex **IV** (33 mg, 4.2 × 10⁻⁵ mol) was mixed with 1,3-diphenylpropanetrione (10 mg, 4.2 × 10⁻⁵ mol) in ~2 mL of dry acetonitrile. The resulting mixture was stirred until everything had dissolved, which gave a light-yellow solution. Aqueous H₂O₂ (4.2 μL of 31% solution, 4.2 × 10⁻⁵ mol) was introduced, and the reaction was stirred for 24 h, during which time the intensity of the yellow color diminished. Sampling of the headspace gas of this reaction mixture indicated the formation of CO/CO₂ in a ~3:1 ratio. Following removal of the solvent under vacuum, the residue was extracted with hexanes/ethyl acetate (1:1) for 1 h, and the soluble portion was brought to dryness (4.4 mg). The species present in this product were identified by ¹H NMR and GC-MS as benzoic acid (major) and small amounts of unreacted 1,3-diphenylpropanetrione and benzil. ¹H NMR analysis of the nickel(II) complex residue indicated the presence of [(6-Ph₂TPA)Ni(sol)₂](ClO₄)₂ (sol = CH₃CN and/or H₂O).¹⁶

Reaction of IV with 1,3-Diphenylpropanetrione, H₂O₂, and NEt₃. Complex **IV** (33 mg, 4.2 × 10⁻⁵ mol) was mixed with 1,3-diphenylpropanetrione (10 mg, 4.2 × 10⁻⁵ mol) in ~2 mL of dry acetonitrile. The resulting mixture was stirred until everything had dissolved, which gave a yellow solution. To this solution was added dry Et₃N (5.9 μL, 4.2 × 10⁻⁵ mol), and the reaction mixture remained yellow. Aqueous H₂O₂ (4.2 μL of 31% solution, 4.2 × 10⁻⁵ mol) was introduced, and the reaction was stirred for 24 h,

(18) Allen, T. H.; Root, W. S. *J. Biol. Chem.* **1955**, *216*, 319–323.

(19) (a) Becke, A. D. *J. Chem. Phys.* **1993**, *98*, 5648–5652. (b) Lee, C.; Yang, W.; Parr, R. G. *Phys. Rev. B* **1988**, *37*, 785–789.

(20) Jaguar, version 7.6; Schrödinger, LLC: New York, 2009.

(21) (a) Tannor, D. J.; Marten, B.; Murphy, R.; Friesner, R. A.; Sitkoff, D.; Nicholls, A.; Honig, B.; Ringnalda, M.; Goddard, W. A., III. *J. Am. Chem. Soc.* **1994**, *116*, 11875–11882. (b) Marten, B.; Kim, K.; Cortis, C.; Friesner, R. A.; Murphy, R. B.; Ringnalda, M. N.; Sitkoff, D.; Honig, B. *J. Phys. Chem.* **1996**, *100*, 11775–11788.

(22) Wolsey, W. C. *J. Chem. Educ.* **1973**, *50*, A335–A337.

during which time the intensity of the yellow color had diminished. Sampling of the headspace gas of this reaction mixture indicated the formation of CO/CO₂ in a ~1.5:1 ratio. Following removal of the solvent under vacuum, the residue was extracted with hexanes/ethyl acetate (1:1) for 1 h, and the slurry was filtered through a Celite plug. The filtrate containing the soluble components was pumped to dryness and found to contain [Et₃NH][ClO₄] and benzil. Washing of the Celite plug with acetonitrile resulted in the elution of the nickel(II) complexes (35 mg). ¹H NMR and MS analysis of this sample indicated the presence of **III** (major) and [(6-Ph₂TPA)Ni(sol)₂](ClO₄)₂ (sol = CH₃CN and/or H₂O; minor).^{11b,16}

Reaction of **I and [Me₄N][PhC(O)C(OH)C(O)Ph] with O₂: Analysis of the Gas Products by GC.** Treatment of a CH₃CN solution of **I** with excess O₂ results in the formation of **III**, benzoic acid, and benzil. Analysis of the headspace gas of this reaction indicated the formation of CO/CO₂ in a ~1.5:1 ratio. Performing a similar headspace gas analysis for the reaction of [Me₄N]-[PhC(O)C(OH)C(O)Ph] with O₂ revealed a primarily CO, with only a trace amount of CO₂.

Results

Complex **I** has been characterized by a number of methods, including single-crystal X-ray crystallography,^{11a} and more recently by X-ray absorption spectroscopy (XAS; see the Supporting Information). The results of these studies indicate that the nickel(II) center in **I** is structurally similar to the ES adduct of Ni^{II}ARD²³ in terms of the ligand composition and overall coordination number but has a slightly longer average Ni–O/N distance (2.16 Å vs 2.04 Å in the ES adduct).

Stopped-Flow Kinetic Studies. As shown in Scheme 2, we have previously reported that the treatment of **I** with O₂ in acetonitrile results in the formation of the monobenzoate complex **III**, benzoic acid, benzil, and CO.^{11b} This reaction has now been examined using stopped-flow kinetic methods. Time-resolved spectra were recorded in the wavelength range of 300–700 nm. In this range, the peak at ~399 nm decreases over time (Figure 1) with a pseudo-first-order rate constant (*k*_{obs}) of 0.0060(3) s⁻¹ at 25 °C. Variation of the concentration of O₂ (Figure S3 in the Supporting Information) revealed a first-order dependence and thus an overall second-order reaction with a rate constant (*k*₂) of 1.7(1) M⁻¹ s⁻¹ at 25 °C (Table 1). Variation of the temperature from +5 to +25 °C and construction of an Eyring plot (Figure S4 in the Supporting Information) yielded Δ*H*[‡] = 7.6(7) kcal/mol and Δ*S*[‡] = -35(4) cal/mol·K.

We have also previously reported that the salt [Me₄N]-[PhC(O)C(OH)C(O)Ph]^{11b} undergoes a reaction with O₂ in CH₃CN to produce tetramethylammonium benzoate, benzoic acid, and CO (Scheme 2, bottom).^{11b,14} We have now monitored this reaction via the disappearance of an absorption band at 385 nm (Figure S5 in the Supporting Information). The reaction is second-order overall (Figure S6 in the Supporting Information) with *k*_{obs} = 0.56(2) s⁻¹ and *k*₂ = 136(3) M⁻¹ s⁻¹ at 25 °C. The reaction was investigated over a 50 °C temperature range, and construction of an Eyring plot (Figure S7 in the Supporting Information) yielded Δ*H*[‡] = 7.9(5) kcal/mol and Δ*S*[‡] = -22(2) cal/mol·K.

Overall, the stopped-flow kinetic studies indicate that the reaction of the monoanion salt [Me₄N][PhC(O)C(OH)C(O)Ph] is ~80 times faster than that of the nickel(II)-

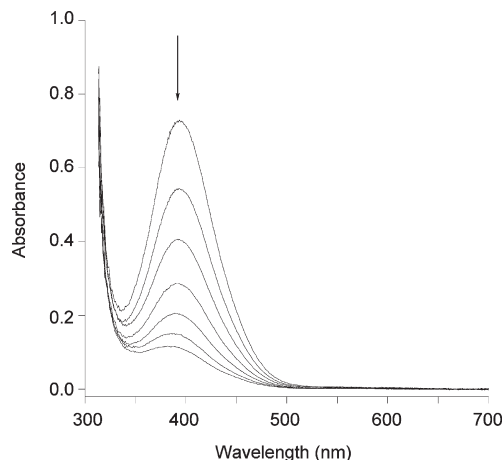


Figure 1. Changes in the absorption spectrum of **I** upon introduction of O₂. Spectra were collected at 20(1) °C at a time interval of 150 s.

Table 1. Rate Constants for the Reactions of the Enolate Complex **I** and [Me₄N][PhC(O)C(OH)C(O)Ph] with O₂ at 25 °C

enolate	<i>k</i> _{obs} (s ⁻¹)	<i>k</i> ₂ (M ⁻¹ s ⁻¹) ^a
I	0.0060(3)	1.7(1)
Me ₄ N[PhC(O)C(OH)C(O)Ph]	0.56(2)	136(3)

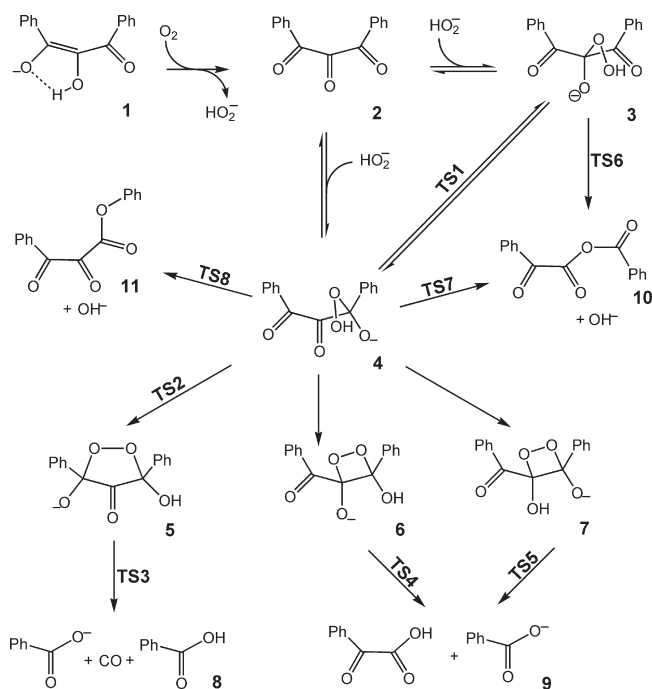
^a[O₂] = 4.1 mM. The *k*₂ value was extrapolated from a plot where *k*_{obs} = *k*₂[O₂].

coordinated anion in **I**. This difference in the reaction rates may be due, in part, to a less favorable activation entropy for the nickel(II)-bound enolate. However, because of the narrow temperature range used for the construction of the Eyring plot for the reaction involving **I** (experimentally limited) and because these reactions are multistep processes and their activation parameters are composite values, we refrain from further comparison and interpretation of the activation parameters.

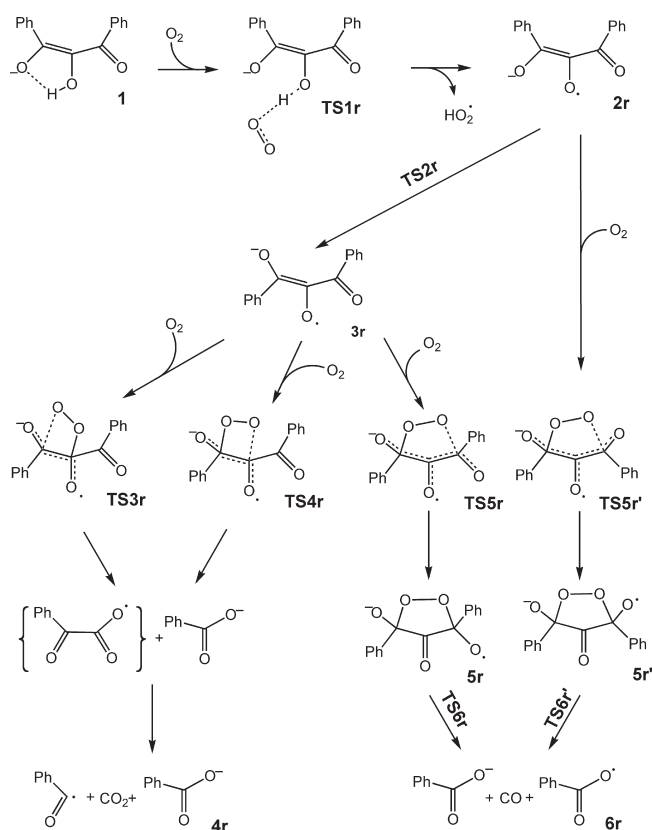
Computational Studies. The nickel(II) complex **I** and the salt [Me₄N][PhC(O)C(OH)C(O)Ph] exhibit similar reactivity with O₂ in terms of the products generated (benzoate salts, benzoic acid, and CO) and the level of ¹⁸O incorporation (Scheme 2). These reactions appear to only differ in terms of the rate of reaction, with the O₂ reaction of the nickel(II) complex being slower, and in the production of the byproduct benzil in the reaction involving **I**. To gain insight into the aliphatic carbon–carbon bond cleavage step, we have performed computational studies on the O₂ reaction of the anion **I**. Two general reaction schemes were considered in modeling the reaction. The first one, termed the hydroperoxide mechanism, is initiated by two-electron oxidation of **I**, and involves the formation of a closed-shell hydroperoxide species (Scheme 4). In the second mechanism, termed the radical mechanism, a one-electron oxidation of **I** is followed by trapping of the resulting radical anion by triplet O₂ (Scheme 5). The calculated energy profiles (Figures 2 and 3) indicate that the hydroperoxide mechanism is most probable, and thus it is described first below. A discussion of the radical path follows. For brevity, we refrain from providing any drawings of the structures in the main text. However, Cartesian coordinates for all stationary points optimized in this work, and pictures of the optimized structures and TSs, can be found in the Supporting Information.

(23) (a) Chai, S. C.; Ju, T.; Dang, M.; Goldsmith, R. B.; Maroney, M. J.; Pochapsky, T. C. *Biochemistry* **2008**, *47*, 2428–2438. (b) Al-Mjeni, F.; Ju, T.; Pochapsky, T. C.; Maroney, M. J. *Biochemistry* **2002**, *41*, 6761–6769.

Scheme 4. Hydroperoxide Mechanism



Scheme 5. Radical Mechanism



Hydroperoxide Mechanism. The key intermediates of the hydroperoxide mechanism are presented in Scheme 4, whereas the free energy profile calculated along the reaction coordinate is shown in Figure 2. For the monoanion **1**, the most stable form corresponds to the species **1**, wherein the central oxygen is protonated and the terminal phenyl

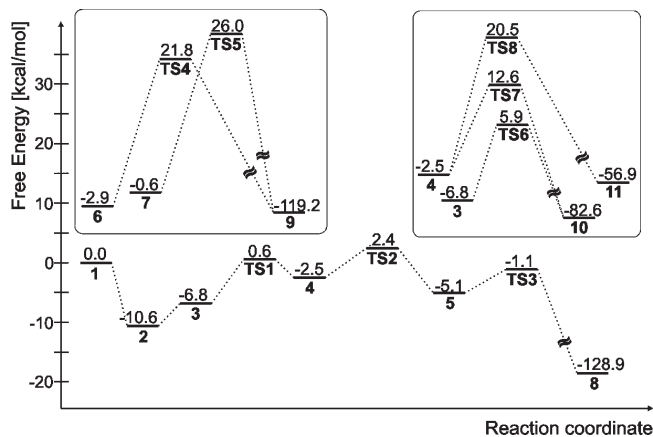


Figure 2. Free energy profile calculated for the hydroperoxide mechanism. The insets show profiles for plausible side reactions.

groups are arranged *cis* with respect to each other (Scheme 4). Other forms of **1**, either with the phenyl groups *trans* or with a proton moved to the peripheral oxygen, are 2.8–9.7 kcal/mol less stable.

A formal hydride transfer from **1** to O_2 yields 1,3-diphenylpropanetrione (**2**) and the hydroperoxide anion. This process is exergonic by 10.6 kcal/mol, and as discussed in the next subsection (*vide infra*), it can be realized as a hydrogen atom transfer from **1** to O_2 , followed by electron transfer between the radical anion **2r** and the hydroperoxy radical.

Formation of the oxygenated products requires that the trione binds HO_2^- , and the most stable form of such an adduct is **3**, which features the hydroperoxide group bound to the central carbon atom. Trapping of HO_2^- by **2** is endergonic by 3.8 kcal/mol, and an additional 4.3 kcal/mol is needed to form an isomer of the hydroperoxide species with the HO_2^- group bound to the side carbonyl (**4**). This intramolecular migration of the HO_2^- anion (**3** \rightarrow **4**) proceeds through a TS (**TS1**) whose free energy, calculated with respect to the separate reactants, is 0.6 kcal/mol. Besides the intramolecular migration of the hydroperoxy group, it is very likely that species **3** and **4** can transform one into another via **2** because the bimolecular reactions involving trione (**2**) and HO_2^- are only modestly endergonic while the corresponding barriers are expected to be small.

The acyclic forms of the adduct, e.g., **3** or **4**, transform into the cyclic peroxo species containing either a four- or five-membered ring (**5**, **6**, or **7**). With calculated free energies of -5.1 , -2.9 , and -0.6 kcal/mol for **5**, **6**, and **7**, respectively, these cyclic intermediates are only slightly less stable than the acyclic predecessor (e.g., **3**) whose calculated free energy is -6.8 kcal/mol. Because of the fact that **6** and **7** are found to be dead-end products (*vide infra*), TSs for their formation, from either **3** or **4**, were not searched for, and only a TS leading to the five-membered ring, e.g., **TS2**, was optimized. Similar to the intramolecular HO_2^- migration (**TS1**), this process (**4** \rightarrow **TS2** \rightarrow **5**) is very facile and involves only a small activation barrier of 2.4 kcal/mol. As can be recognized from the structure of **TS2** (see the Supporting Information), this ring-closure reaction consists of concerted, yet asynchronous, proton transfer and formation of the C–O bond. Indeed, in **TS2**, the distance between the proton and acceptor oxygen is only 1.18 Å, whereas the C–O separation is 2.75 Å. However, once **TS2** is passed,

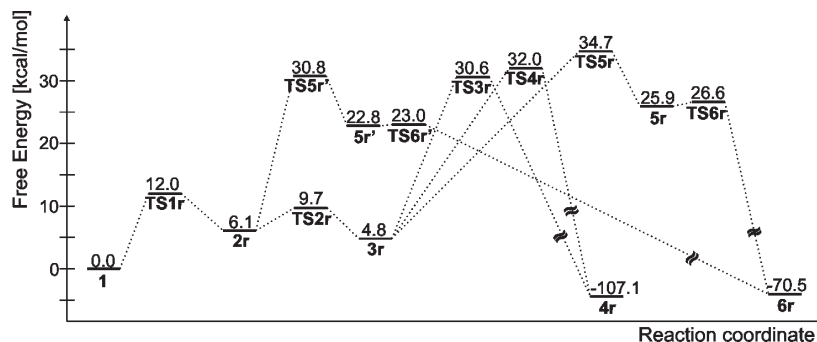


Figure 3. Free energy profile calculated for the radical mechanism.

the C–O bond develops without any additional barrier. Importantly, as can be recognized in Figure 2, **TS2** is the highest point on the free energy profile joining **2** and the CO-extrusion products, i.e., **8**. Thus, an accumulated barrier (**2** → **TS2**) for this reaction is associated with **TS2**, and it amounts to 13.0 kcal/mol. In other words, formation of the cyclic peroxo species with a five-membered ring (**5**) is predicted to be the rate-limiting step in the reaction of 1,3-diphenylpropanetrione (**2**) and HO_2^- .

Species **5** is a very reactive intermediate that easily decomposes with the release of the benzoate anion, benzoic acid, and CO. The calculated free energy for the TS connected with this process (**TS3**) is -1.1 kcal/mol, which is only 4 kcal/mol more than the energy for the cyclic intermediate **5**. Notably, both the structure of **TS3** and its low energy are very similar to those found for the final step of the catalytic cycle of quercetin 2,3-dioxygenase.²⁴

In terms of the chemistry of acireductones, it is interesting to examine the properties of a cyclic peroxo species with a four-membered ring (**6** or **7**) from which aliphatic carbon–carbon bond cleavage could yield a α -keto acid and a monocarboxylic acid. This is the reaction observed for the native acireductone substrate in the absence of an enzyme.⁶ For the O_2 addition product of **1**, two tautomers need to be considered: one with the peripheral oxygen bearing a proton (**6**) and the second where the central oxygen is protonated (**7**). The free energies of these structures are not prohibitively high, -2.9 and -0.6 kcal/mol, respectively, and thus it seems likely that such four-membered rings can form. Yet, cleavage of the O–O and C–C bonds in these intermediates, which leads to products including a α -keto acid (**9**), is a difficult process. Free energy values calculated for TSs connected with this reaction (**TS4**, 21.8 kcal/mol, **TS5**, 26.0 kcal/mol) are more than 20 kcal/mol higher than those for **TS3** (-1.1 kcal/mol), and thus, it is safe to conclude that at ambient temperature this reaction channel will not be used because all of the substrate will react via **TS3**. It seems appropriate to mention here that the high energy of **TS4** and **TS5** is not an artifact caused by the use of a restricted wave function. The calculations were repeated in the unrestricted regime, but no solutions with lower energy could be found.

Importantly, both types of cleavage reaction, leading to either CO extrusion (**8**) or formation of α -keto acid (**9**), are highly exergonic, with the calculated free energy amounting to -128.9 and -119.2 kcal/mol, respectively. This large exergonicity implies that decomposition of the

cyclic peroxide species is practically irreversible, and as a consequence, the identity of the reaction products is controlled by the barriers (kinetic reaction control).

Yet another reaction channel that can be envisioned for the decay of the peroxide intermediates involves a Baeyer–Villiger rearrangement. In this case, migration of a carbonyl group to the peroxo oxygen leads from the acyclic hydroperoxide **3** or **4** to the keto acid ester **10**, which upon hydrolysis decomposes to the same products as those obtained via **TS4** or **TS5**, i.e., **9**. The free energies obtained for optimized TSs for acyl migrations, **TS6** and **TS7**, are 5.9 and 12.6 kcal/mol, respectively, which are at least 3.5 kcal/mol higher than the energy of **TS2**, which is the highest point on the free energy profile, leading to the CO-extrusion products **8**. Thus, only a modest free energy gap of 3.5 kcal/mol spans the critical TSs (**TS2** and **TS6**), controlling the decay through two different reaction channels, and it seems plausible that, by appropriate modification of the reactants and/or reaction conditions, the product specificity might be altered.

Finally, for the acyclic peroxide species **4**, a Baeyer–Villiger rearrangement with migration of the phenyl group leads through **TS8** to a phenol ester **11**. However, the calculated free energy for this TS is as high as 20.5 kcal/mol, which makes this process very unlikely.

Radical Mechanism. In the previous theoretical investigations of the aqueous solution reaction between the native acireductone monoanion $[\text{RC}(\text{O})\text{C}(\text{OH})\text{CHO}]^-$ ($\text{R} = \text{alkyl}$) and O_2 , it was found that a radical mechanism is most likely involved in the production of the observed products, which are a α -keto acid and formate.¹⁰ Therefore, it was natural to test such a reaction mechanism for the current enolate, and the results are summarized in Scheme 5 and Figure 3. At the outset of the radical mechanism, the monoanion **1** is oxidized by O_2 via a direct hydrogen atom transfer between the reactants (**TS1r**). The calculated free energy for this TS is 12.0 kcal/mol, and because **TS1r** is the highest point on the reaction path leading to the radical anion in its most stable configuration (**3r**), this step is rate-limiting for its production. For the radical-anion intermediate, the lowest-energy conformation corresponds to the structure with two phenyl groups trans to each other (**3r**). Rotation around the partial double bond C–C, which transforms **2r** into **3r**, involves a rather small activation barrier (3.6 kcal/mol) connected with **TS2r**.

Before further steps of the radical mechanism are discussed, it should be mentioned that the reaction steps leading from **1** to **3r** can also constitute an initial stage of the hydroperoxide mechanism discussed above. More

(24) Siegbahn, P. E. M. *Inorg. Chem.* **2004**, *43*, 5944–5953.

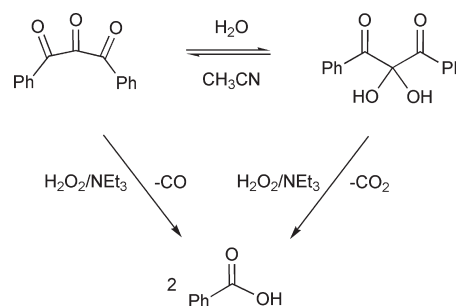
specifically, the radical ion **3r** can react with the hydroperoxide radical, producing either trione **2** and HO_2^- or the hydroperoxide species **3** or **4** directly. Even though the structure of a TS connected with such an electron-transfer process has not been found, it is expected that the activation free energy approximately equals the entropy term of HO_2^\bullet trapping (~ 10 kcal/mol). This is based on an assumption that the enthalpy barrier for such an exergonic electron transfer ($3\mathbf{r} + \text{HO}_2^\bullet \rightarrow 2 + \text{HO}_2^-$; $\Delta G = -15.2$ kcal/mol) is most likely negligible. Thus, the two-electron oxidation of **1** yielding **2** and HO_2^- is proposed to proceed through a TS whose estimated free energy is 14.8 kcal/mol (4.8 kcal/mol for **3r** plus 10 kcal/mol from the entropy term). Importantly, this value matches well with the free energy of activation determined experimentally ($\Delta G^\ddagger = 14.4(8)$ kcal/mol) via stopped-flow kinetic studies of the reaction of the anion **1** with O_2 .

Radical anion **3r** can react with O_2 in three different ways, corresponding to three TSs: **TS3r**, **TS4r**, and **TS5r**. In addition, when **2r** reacts with O_2 , an isomeric TS, i.e., **TS5r'**, is involved. The first two pathways yield the products involving an unstable keto acid radical, which decomposes with the release of CO_2 (**4r**), whereas **TS5r** and **TS5r'**, with a five-membered ring, lead eventually to CO -extrusion products (**6r**). **TS3r** and **TS4r** differ in the site of the primary attack of O_2 . In **TS3r**, the attack occurs in such a way that the central carbon is most advanced in developing a bond with O_2 , whereas in **TS4r**, it is the peripheral carbon that forms the C–O bond faster. Notably, the calculated free energies for these TSs are very high, amounting to 30.6, 32.0, 34.7, and 30.8 kcal/mol, for **TS3r**, **TS4r**, **TS5r**, and **TS5r'**, respectively, which when compared to the barriers found in the hydroperoxide mechanism, clearly shows that the reaction between O_2 and **3r** or **2r** is unlikely.

Taking into account the prohibitively high barriers found for the radical mechanism and the fact that for the native acireductone it is the radical mechanism that was previously suggested for its uncatalyzed reaction with O_2 ,¹⁰ an interesting question arises as to the origin of the difference in the reactivity of native acireductone and the phenyl-substituted analogue investigated in this work. When the structures and energies of **TS3r**, **TS4r**, and **TS5r** were compared with those found previously for the native acireductone,¹⁰ it was noticed that low-barrier TSs are those where the aldehyde carbon, present in natural acireductone, is the site of the primary attack of O_2 . For example, for the two TSs resembling **TS5r**, the calculated free energies are 19.8 and 27.7 kcal/mol, where the lower barrier is for the TS with the aldehyde carbon as the site of the primary attack of O_2 . Even larger differences were found for TSs corresponding to **TS4r** and **TS3r** because the two free energy values are 12.6 and 26.1 kcal/mol, with the latter quite close to the 25.8 kcal/mol difference between the energies of **3r** and **TS3r** calculated in this work. In summary, in the low-barrier radical paths, it is the aldehyde carbon that is attacked first by O_2 , and the lack of such a functional group makes the radical mechanism unattainable for the acireductone compound **1** investigated in this work.

Independent Reactions Involving 1,3-Diphenylpropanetrione. The computational studies suggest the involvement of 1,3-diphenylpropanetrione and HOO^- as intermediates, leading to aliphatic carbon–carbon bond cleavage in the

Scheme 6

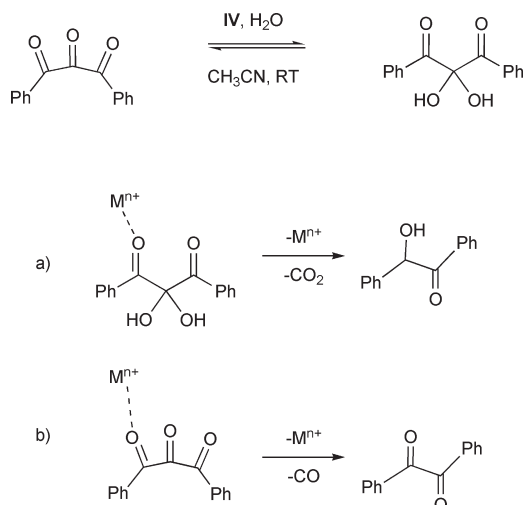


reaction of **1** with O_2 . Therefore, we have independently investigated the reactivity of 1,3-diphenylpropanetrione with H_2O_2 (1 equiv, 31% solution) upon stirring in CH_3CN for 24 h. The species identified by ^1H NMR in the final reaction mixture were unreacted 1,3-diphenylpropanetrione ($\sim 57\%$), hydrated 1,3-diphenylpropanetrione ($\sim 7\%$), and benzoic acid ($\sim 36\%$). The addition of NEt_3 to the reaction mixture enabled the formation of the HOO^- anion and significantly enhanced the amount of benzoic acid/benzoate generated ($\sim 70\%$ yield). In both of these reactions, examination of the headspace gas by GC indicated the formation of CO and CO_2 in a $\sim 12:1$ ratio. The outcomes of these reactions are consistent with the formation of cyclic peroxide species akin to **5** (Scheme 4) and its hydrated form (Scheme 6), which then undergo aliphatic carbon–carbon bond cleavage to give benzoic acid/benzoate. The high ratio of CO/CO_2 can be attributed to the higher oxidative cleavage reactivity for the trione versus the hydrated triketone. The former has a more electrophilic central carbon to which OOH^- addition occurs.

In the reaction of **1** with O_2 , in addition to the formation of benzoic acid/benzoate and CO as products, we have previously identified the production of benzil.^{11b} We hypothesized that this byproduct was due to the formation of 1,3-diphenylpropanetrione and a solvated nickel(II) complex such as $[(6\text{-Ph}_2\text{TPA})\text{Ni}(\text{sol})_2](\text{ClO}_4)_2$ in the reaction mixture, with the latter serving as a Lewis acid to promote migration chemistry involving the trione. To evaluate this idea, we stirred **IV** and 1,3-diphenylpropanetrione in dry acetonitrile for 6 h. At this point, approximately 50% of 1,3-diphenylpropanetrione had reacted to give hydrated 1,3-diphenylpropanetrione ($\sim 7\%$) and benzil and benzoin (combined yield $\sim 30\text{--}35\%$; Figure S8 in the Supporting Information). Evaluation of the headspace gas of the reaction mixture using GC indicated the formation of CO_2 , with very little CO generated ($\sim 1:10$ CO/CO_2). On the basis of literature precedent,²⁵ as shown in Scheme 7, we propose that the nickel(II) center of **IV** promotes the formation of hydrated trione and the loss of CO_2 from this molecule via a benzoyl migration reaction (Scheme 7a). The formation of CO occurs from 1,3-diphenylpropanetrione via a similar migration reaction (Scheme 7b). It is known that Lewis acids such as AlCl_3 promote decarbonylation of 1,3-diphenylpropanetrione with a loss of the central carbonyl carbon, as shown by ^{14}C -labeling studies.²⁵ If water is present in the AlCl_3 -promoted reaction, benzoin and CO_2 are instead

(25) Roberts, J. D.; Smith, D. R.; Lee, C. C. *J. Am. Chem. Soc.* **1951**, *73*, 618–625.

Scheme 7



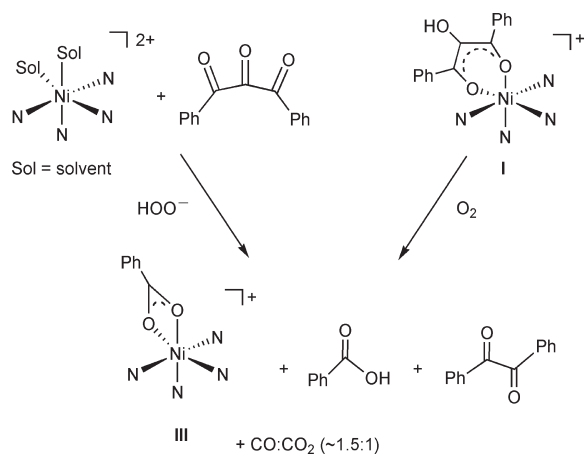
generated, with this reaction involving a hydrated form of the trione.

The addition of H_2O_2 to the reaction shown in Scheme 7 (top) and stirring for 24 h result in the formation of benzoic acid as the major organic product, with small amounts of unreacted 1,3-diphenylpropanetrione, hydrated 1,3-diphenylpropanetrione, and benzil also present. The headspace gas was found to contain both CO and CO_2 . The only nickel(II) complex present at the end of the reaction is a solvate complex, $[(6\text{-Ph}_2\text{TPA})\text{Ni}(\text{sol})_2](\text{ClO}_4)_2$ ($\text{sol} = \text{CH}_3\text{CN}$ or H_2O). These combined results suggest a reaction pathway wherein the trione can undergo direct reaction with H_2O_2 to yield aliphatic carbon–carbon bond cleavage reactivity (benzoic acid) or migration chemistry to give benzil. The formation of CO_2 suggests that benzoin is also formed in the reaction mixture from hydrated trione. However, in the presence of H_2O_2 , benzoin would be oxidized to benzil. If 1 equiv of NEt_3 is added to the mixture of IV, 1,3-diphenylpropanetrione, and H_2O_2 , similar products are obtained albeit the primary metal-containing product is now the nickel(II) benzoate complex III and the CO/CO_2 ratio is $\sim 1.5:1$. Similarly, III is the primary metal complex product generated in the reaction of I with O_2 . To further compare the nickel(II) complex/trione/ $\text{H}_2\text{O}_2/\text{NEt}_3$ reactivity with that of I and O_2 , we have examined the gaseous products generated in the latter reaction using GC. This experiment revealed a CO/CO_2 ratio of $\sim 1.5:1$, which is similar to that noted above for the nickel(II) complex/trione/ $\text{H}_2\text{O}_2/\text{NEt}_3$ reaction. Overall, these combined results provide strong evidence that the reaction of I with O_2 likely proceeds via a trione/ HOO^- pathway because both reactions give similar products (Scheme 8).^{11b}

Discussion

The discovery of ARDs and Dkel has sparked interest in elucidating the O_2 reactivity of metal-coordinated enolate/enediolate ligands. In the ES adducts of both $\text{Ni}^{\text{II}}\text{ARD}$ and Dkel, the substrate is proposed to bind to the active site metal center as a 1,3-chelate ligand,^{3,6,9} with the former substrate having a deprotonated hydroxyl moiety at the C(2) carbon. With regard to substrate specificity, the Dkel enzyme will catalyze the oxidative cleavage of a variety of acetylacetonate

Scheme 8



derivatives substituted at the 1, 3, or 5 position to yield the corresponding carboxylic acids and α -keto aldehydes.³ Studies of $\text{Ni}^{\text{II}}\text{ARD}$ have shown that acireductones having a C(1)–H bond and an alkyl or aryl substituent at the C(3) position (Scheme 1c) can serve as substrates for the enzyme.²⁶ For both $\text{Ni}^{\text{II}}\text{ARD}$ and Dkel, a mechanistic pathway is proposed wherein O_2 activation occurs at the enolate/enediolate ligand and results in the formation of a coordinated cyclic peroxo-containing ligand from which aliphatic carbon–carbon bond cleavage occurs. To date, model studies that address the mechanism of aliphatic carbon–carbon bond cleavage reactivity in synthetic complexes of relevance to these enzymes are lacking. Recently, a reactive model complex for Dkel has been reported wherein an iron(II) complex containing a 3-phenyldiethylmalonate (Phmal) ligand, $[\text{Tp}^*\text{Fe}(\text{Phmal})]$ [$\text{Tp}^* = \text{hydridotris}(3,5\text{-dimethylpyrazol-1-yl})\text{-borato}$], was shown to undergo oxidative carbon–carbon bond cleavage upon exposure to O_2 .²⁷ Oxidation of $[\text{Tp}^*\text{Fe}(\text{Phmal})]$ with NOPF_6 to generate an iron(III) complex, followed by exposure to O_2 , resulted in no carbon–carbon bond cleavage reactivity. Therefore, it was suggested that iron(II) is required for O_2 activation, and a proposed mechanism was put forth wherein the initially formed iron(III) superoxide species attacks an electrophilic carbonyl carbon atom to give an iron organoperoxide unit. From this species, dioxetane could form or O–O bond cleavage could occur to give a high-valent iron oxo species. Either of these species could undergo further reaction to give the observed reaction products. Detailed mechanistic studies of this reaction have not yet been reported. A previously reported study of the O_2 -induced C(2)–C(3) bond cleavage of iron(II)-coordinated phenylpyruvate ligands invoked a mechanism wherein O_2 interacts with the C(3) carbon of the coordinated enolate and not the iron(II) center.²⁸

As an approach toward generating a synthetic complex of relevance to the ES adduct of $\text{Ni}^{\text{II}}\text{ARD}$, we previously prepared I and characterized this complex by multiple methods, including single-crystal X-ray crystallography. To facilitate comparison to the enzyme ES adduct, in the

(26) (a) Myers, R. W.; Wray, J. W.; Fish, S.; Abeles, R. H. *J. Biol. Chem.* **1993**, *268*, 24785–24791. (b) Wray, J. W.; Abeles, R. H. *J. Biol. Chem.* **1993**, *268*, 21466–21469. (c) Dai, Y.; Pochapsky, T. C.; Abeles, R. H. *Biochemistry* **2001**, *40*, 6379–6387.

(27) Siewert, I.; Limberg, C. *Angew. Chem., Int. Ed.* **2008**, *47*, 7953–7956.

(28) Paine, T. K.; England, J.; Que, L., Jr. *Chem.—Eur. J.* **2007**, *13*, 6073–6081.

research reported herein we have further characterized this complex by XAS. Similar to the ES adduct in Ni^{II}ARD, **I** has a six-coordinate nickel(II) center with a primary coordination environment comprised of O/N donors. The synthetic complex has a longer average Ni–O/N distance (2.16 Å) than is found for the enzyme ES adduct (2.04 Å),²⁹ with the longest Ni–N distances in **I** involving the phenyl-appended pyridyl donors. These appendages create a hydrophobic microenvironment, within which the enolate **I** is coordinated to the nickel(II) center. In the secondary environment of Ni^{II}ARD, two phenylalanine residues are proposed to orient coordination of the acireductone to the nickel(II) center.⁶ Thus, complex **I** mimics the key features of both the primary and secondary coordination environment of the Ni^{II}ARD ES adduct.

In our research, we have used [PhC(O)CH(OH)C(O)Ph][–] (Scheme 2) as a model for the native acireductone monoanion substrate in Ni^{II}ARD. The presence of the phenyl group at the C(1) position of this anion has important influences on the chemistry. The computational studies outlined herein provide a rationale for why this anion, upon reaction with O₂, undergoes oxidative cleavage of the C(1)–C(2) and C(2)–C(3) bonds with extrusion of CO/CO₂ instead of C(1)–C(2) cleavage, as is found for C(1)–H acireductones. While four-membered cyclic peroxide species can form (two different tautomers possible) upon reaction of **I** with O₂, cleavage of the O–O and C–C bonds in these intermediates, which would lead to products akin to those found for a C(1)–H acireductone (α -keto acid and formate), is an unfavorable process. Specifically, the TSs associated with such a reaction are more than 20 kcal/mol higher than the TSs for C(1)–C(2) and C(2)–C(3) in a five-membered cyclic peroxide. Thus, **I** is predisposed to undergo CO-extrusion chemistry upon reaction with O₂, whereas the native C(1)–H acireductone and analogues can exhibit differing oxidative carbon–carbon reactivity depending on the nature of metal in the enzyme.⁸ This issue is the key feature of the chemistry of ARD enzymes, as shown in Scheme 2, wherein the coordination mode of a C(1)–H acireductone has been proposed to determine the outcome of the aliphatic carbon–carbon bond cleavage reaction.⁹

Another consequence of the C(1)–Ph group in **I** is that the TS barriers associated with the formation of a cyclic peroxide structure via a radical reaction pathway, as has been proposed for the aliphatic carbon–carbon bond cleavage reactivity of a C(1)–H acireductone,¹⁰ are prohibitively high. Instead, computational studies suggest that the reaction of **I** with O₂ proceeds via a hydroperoxide mechanism with 1,3-diphenylpropanetrione and HOO[–] as intermediates. Independent reactions between the trione and OOH[–] in the presence of a nickel(II) complex, and examination of the products of these reactions, provided evidence that a trione pathway akin to that shown in Scheme 3 (pathway B) is feasible for the reaction of **I** with O₂. For example, the similarity of the product distribution, including CO/CO₂ ratios, suggests that both reactions proceed via a similar pathway (Scheme 8). Additionally, a trione pathway provides an explanation for how benzil is generated in the reaction mixture. Lewis acid-promoted

benzoyl migration chemistry involving 1,3-diphenylpropanetrione, or its hydrated form, will give benzil/CO or benzoin/CO₂, respectively. Our work demonstrates that, in a trione-type reaction pathway for oxidative cleavage of an acireductone, the amount of CO generated relative to CO₂ depends on the reaction conditions, specifically the water content of the reaction and the presence of a metal ion.

Kinetic studies revealed that coordination of the anion **I** to nickel(II) in **I** significantly slows the reaction with O₂, with the free anion reacting ~ 80 times faster at 25 °C. The slower rate of reaction for **I** appears to result, at least in part, from a less favorable activation entropy, which is perhaps due to the presence of the bulky 6-Ph₂TPA ligand. However, it is worth noting that the difference in the rate between free and nickel(II)-coordinated **I** is similar to that seen between the mono- and dianionic forms of the *n*-propyl acireductone in aqueous solution (0.12 and 8 M^{–1} s^{–1}, respectively; ~ 66 times faster for the dianion).³⁰ These combined results suggest that the relative reactivity of the enolate is related to its effective charge. The anion **I** is expected to be a better reductant toward O₂ than the nickel(II)-coordinated enolate in **I** because of the electron-withdrawing effect of the nickel(II) center. Similarly, the more electron-rich *n*-propyl acireductone dianion should be a better reductant than the corresponding monoanion. To date, no kinetic studies have been reported for the reaction of a nickel(II)-coordinated acireductone dianion with O₂. Using multinuclear nickel(II) enediolate complexes generated in our laboratory, we are pursuing such investigations.

One final note regarding the kinetic studies presented herein is that the reactions of **I** and **I** with O₂ both proceed via similar trione/HOO[–] mechanisms, which enables a clear comparison of the rate constants. This is not the case for the reactions of a free versus nickel(II)-coordinated C(1)–H acireductone with O₂. These reactions are known to yield different products, albeit both may proceed with a similar rate-determining step involving an initial electron transfer from enolate/enediolate to O₂.

At first glance, slowing of the reaction in the presence of the nickel(II) center may seem counterintuitive with regard to the enzymatic reaction. However, the role of the nickel(II) center in the enzymatic reaction is to act as a Lewis acid to ensure that a supply of the deprotonated form of the substrate is available at neutral pH because the protonated form is not reactive with O₂. This is similar to the chemistry of Zn–OH species in biological systems.³¹ A Zn–OH moiety is a poorer nucleophile than free OH[–], but the concentration of free OH[–] at pH 7 is very low. In both Ni^{II}ARD and zinc hydrolytic enzymes, the metal center acts as a Lewis acid to ensure that the reactive species is available in sufficient quantity at neutral pH.

Conclusions

The research outlined herein reveals that while **I** has structural relevance to the Ni^{II}ARD ES adduct, the O₂-dependent oxidative carbon–carbon bond cleavage and CO-extrusion reaction proceeds via a hydroperoxide/trione-type mechanism (Scheme 3, pathway B). This reaction pathway differs from that proposed for the Ni^{II}ARD enzyme reaction and is due to the presence of a phenyl appendage at the C(1) carbon of **I**. Thus, at least two mechanistic pathways for oxidative carbon–carbon bond cleavage and CO extrusion are possible from an acireductone-type ligand, with the

(29) (a) Pochapsky, T. C.; Pochapsky, S. S.; Ju, T.; Mo, H.; Al-Mjeni, F.; Maroney, M. J. *Nat. Struct. Biol.* **2002**, *9*, 966–972. (b) Pochapsky, T. C.; Pochapsky, S. S.; Ju, T.; Hoefler, C.; Liang, J. J. *Biomol. NMR* **2006**, *34*, 117–127.

(30) Berreau, L. M. *Adv. Phys. Org. Chem.* **2006**, *41*, 79–181.

(31) Wray, J. W.; Abeles, R. H. *J. Biol. Chem.* **1995**, *270*, 3147–3153.

differentiation resulting from the nature of the C(1) substituent of acireductone.

In terms of synthetic bioinorganic chemistry, this work demonstrates that, in the design of reactive model complexes for metal sites in biomolecules, it is very important to consider not only the amino acid ligand sphere of the metal center but also the chemical features of the substrate analogue that is employed if the native substrate is not available.

Acknowledgment. Funding for this research was provided by the National Science Foundation (Grant CHE-0848858 to L.M.B. and Grant CHE-0750140 to E.V.R.-A.). Stopped-flow instrumentation at Tufts University was

supported by the NSF CRIF program (Grant CHE-0639138). T.B. thanks the Polish Ministry of Science and Higher Education (MNiSW) for supporting this research project (Grant N301 093036).

Supporting Information Available: Details of XAS studies; plots of the O₂ dependence of k_{obs} for **I** and **1**; absorption versus wavelength plot for the reaction of **1** with O₂; Eyring plots; Cartesian coordinates, electronic energies, and pictures of the optimized structures/Ts along the reaction coordinates; ¹H NMR of organic products generated in the reaction of [(6-Ph₂TPA)Ni(CH₃CN)(H₂O)](ClO₄)₂ with 1,3-diphenylpropanetrione. This material is available free of charge via the Internet at <http://pubs.acs.org>.